

Homography-Based Multi-Robot Control with a Flying Camera

G. López-Nicolás¹, Y. Mezouar² and C. Sagüés¹

Abstract—This paper addresses the problem of visual control of a set of mobile robots. In our framework, the perception system consists of a calibrated flying camera looking downward to the mobile robots. The robots are assumed to undergo planar motion considering nonholonomic constraints. The goal of the task is to control the multi-robot system to a desired configuration relying solely on visual information given by the flying camera. The desired multi-robot configuration is defined with an image of the set of robots in that configuration. Then, any arbitrary configuration can be easily defined by this image without any additional information. As contribution, a new image-based control scheme is presented relying on the homography induced by the multi-robot system to lead the robots to the desired configuration. The stability of the control law is analyzed and simulations are provided to illustrate the proposal.

I. INTRODUCTION

Nowadays, multi-robot systems are an important research area in robotics. It is known that a multi-robot system can perform tasks that are difficult for one single robot like exploration, surveillance, security or rescue operations. One of the research topics in this area is the problem of reaching and maintaining the robot team in a particular configuration [1] [2] [3].

Visual information has been extensively used for robot localization, navigation and control. Visual control is an extensive field of research in the design of motion controllers and it has focused the attention of many researchers [4]. It is usual in multi-robot systems that each robot is equipped with a local perception system to accomplish the global task sharing their information. See for example the localization method for multiple mobile robots presented in [5]. Another related work is [2], that aims to enable groups of mobile robots to visually maintain formations, but they go a step further by considering the problem in the absence of communication between the robots. The issue of switching between decentralized and centralized cooperative control is tackled in the vision-based formation control with feedback-linearization proposed in [1].

Some of the advantages of using a centralized approach is that it allows simple and cheap robots, and releases their local resources transferring expensive computations to an external computer. A centralized architecture is considered for the leader-follower control proposed in [3], where the perception

system consists of a fixed camera on the ceiling. In general, visual information is more robust if multiple view geometry constraints are imposed [6]. In particular, the homography is a well-known geometric model across two views induced by a plane of the scene, and it has been used extensively in visual control [7], [8], [9].

In the framework considered here, the multiple robots are assumed to move in a planar surface and constrained to non-holonomic motion. The goal of the control scheme proposed is to drive the multiple robots to a desired configuration defined by an image previously taken of that configuration. The visual information is acquired by a flying camera looking downward that undergoes an arbitrary planar motion, in such a way that its translation is parallel to the robots motion plane and the rotation is parallel to the plane normal.

We propose a homography-based control approach that takes advantage of the planar motion constraint to parametrize the homography. This particular parametrization makes the approach feasible for a set of two or more robots. The image features to compute the homography are the projection of the multiple robots on the image plane. Then, the homography computed gives information about the configuration of the set of robots. In particular, it can be known if the configuration of the robots is rigid, i.e. they maintain the desired configuration defined by the target image, or nonrigid, meaning that the robots are in a different configuration to the one desired. A new image-based control law is proposed where a desired homography is defined as a reference for the control in order to drive the robots to the desired configuration. This approach is different than other image-based techniques in the use of the homography for multi-robot formation. In particular, this homography is the way to handle the interaction between the robot team.

The main contributions are the homography-based framework, that gives a desired homography to define the reference target, and the image-based control law that drives the robots to the desired configuration. The advantages of the approach presented are that any arbitrary desired configuration can be easily defined with one image, avoiding the need of additional information like 3D measurements or relative positions between the robots. Another advantage of the approach is that the camera does not need to be static. Notice that the camera can freely move while carrying out different or additional tasks independently of the control task. Moreover, the motion of the camera is an arbitrary planar motion unknown to the control scheme without affecting the control performance.

The paper is organized as follows. Section II presents the parametrization of the homography and the definition of the desired homography for reaching the multi-robot goal

¹ Instituto de Investigación en Ingeniería de Aragón. Universidad de Zaragoza, Spain. {gonlopez, csagues}@unizar.es

² LASMEA - Université Blaise Pascal, Aubiere 63177, France. youcef.mezouar@lasmea.univ-bpclermont.fr

This work was supported by "Programa Europa XXI de la Comisión Mixta Caja de Ahorros de la Inmaculada - CONAI+D del Gobierno de Aragón", project DPI2009-08126, and the ANR R-discover project.

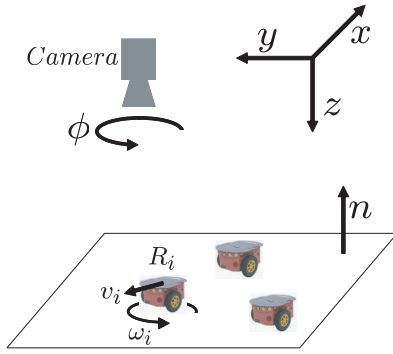


Fig. 1. Coordinate system: The motion of the camera occurs in the $x - y$ plane of the global reference and the robots undergo planar motion parallel to the $x - y$ plane. The rotation of the camera is also parallel to the plane normal \mathbf{n} .

configuration. The control law for the multi-robot system is presented in section III including the stability analysis of the control scheme. Simulations are given in Section IV to illustrate the performance of the proposal. Section V presents the conclusions of the paper.

II. HOMOGRAPHY-BASED SCHEME

The setup of the multi-robot system and the flying camera is illustrated in Fig. 1, where the global fixed Left-handed coordinate system is depicted. In the following, we parametrize the homography in this framework and describe the method to compute linearly the homography. Then, we propose a procedure to define the desired homography that corresponds to the desired configuration of the multi-robot system.

A. Homography Parametrization

Two perspective images can be geometrically linked through a plane by a homography $\mathbf{H} \in \mathbb{R}^{3 \times 3}$. This projective transformation \mathbf{H} relates points of the plane projected in both images. Pairs of corresponding points $(\mathbf{p}, \mathbf{p}')$ are then related up to scale by $\mathbf{p}' = \mathbf{H}\mathbf{p}$. The calibrated homography can be related to camera motion and plane parameters as follows

$$\mathbf{H} = \mathbf{R} + \mathbf{T}\mathbf{n}^T/d, \quad (1)$$

where \mathbf{R} and \mathbf{T} are the relative rotation and translation of the camera, \mathbf{n} is the unit normal of the plane with respect to the reference frame and d is the distance along \mathbf{n} between the plane and the reference position. In the framework considered, the position of the camera $(x, y, z)^T$ is constrained to the plane $x - y$ (i.e. $z = 0$) and rotation ϕ about the z -axis. This constraint yields

$$\mathbf{R} = \begin{bmatrix} \cos \phi & \sin \phi & 0 \\ -\sin \phi & \cos \phi & 0 \\ 0 & 0 & 1 \end{bmatrix}, \quad \mathbf{T} = \begin{pmatrix} t_x \\ t_y \\ t_z \end{pmatrix}, \quad (2)$$

with $\mathbf{T} = -\mathbf{R}(x, y, 0)^T$.

In our framework, the mobile robots move in a planar surface that generates the homography. Besides, the camera undergoes planar motion: the translation is parallel to the plane and the rotation is parallel to the plane normal, i.e. the z -axis, and $\mathbf{n} = (0, 0, -1)^T$. Notice that the distance d is the

height of the camera with respect the motion plane of the robots. Therefore, the homography matrix is given by

$$\begin{aligned} \mathbf{H} &= \begin{bmatrix} h_{11} & h_{12} & h_{13} \\ h_{21} & h_{22} & h_{23} \\ 0 & 0 & 1 \end{bmatrix} \\ &= \begin{bmatrix} \cos \phi & \sin \phi & -t_x/d \\ -\sin \phi & \cos \phi & -t_y/d \\ 0 & 0 & 1 \end{bmatrix}. \end{aligned} \quad (3)$$

B. Homography Computation

The homography across two views can be computed from a minimal set of four point correspondences solving a linear system [10]. In our framework, the points considered consist of the projection of the robots on the image plane, and they are denoted in homogeneous coordinates by $\mathbf{p} = (p_x, p_y, 1)$. A point correspondence $(\mathbf{p}, \mathbf{p}')$ is related up to scale by the homography as $\mathbf{p}' = \mathbf{H}\mathbf{p}$, which can be expressed in terms of the vector cross product as $\mathbf{p}' \times \mathbf{H}\mathbf{p} = \mathbf{0}$ [10]. From this expression two linearly independent equations in the entries of \mathbf{H} (3) are obtained

$$\begin{bmatrix} p_x & p_y & 1 & 0 & -p'_x \\ p_y & -p_x & 0 & 1 & -p'_y \end{bmatrix} \begin{pmatrix} h_{11} \\ h_{12} \\ h_{13} \\ h_{23} \\ h_{33} \end{pmatrix} = 0. \quad (4)$$

Each point correspondence gives two independent equations. Given that \mathbf{H} is defined by seven unknown entries, and using the homography constraints $h_{11} = h_{22}$ and $h_{21} = -h_{12}$, a set of two point correspondences allows to determine the homography up to a scale factor by solving a linear system. Given that h_{33} is never zero because of the particular form (3), the scale of the homography can always be normalized and fixed by this entry.

C. The Target Homography

Each pair of robots induce a homography across two images, the current image and the image of the desired configuration. Given a set of N robots, the number of homographies defined by the different pair of robots is $N(N - 1)/2$. If all of these homographies are equal, the relative motion of the robots is rigid. Otherwise, if any of the homographies is different to the others, the relative motion of the set of robots is not rigid and they are not in the desired configuration. A desired homography computed using all robots needs to be defined in order to lead the robots to the desired configuration.

In the first case, the homography induced by the plane of the robots moving in the desired configuration is conjugate to a planar Euclidean transformation given by

$$\mathbf{H}_{rigid} = \begin{bmatrix} \cos \phi & \sin \phi & h_{13} \\ -\sin \phi & \cos \phi & h_{23} \\ 0 & 0 & 1 \end{bmatrix}. \quad (5)$$

Notice that the upper left hand 2×2 matrix is orthogonal. The Euclidean transformation produces a translation and rotation

of the image, and lengths and angles are invariants by this transformation.

The angle of rotation is encapsulated in the eigenvalues of (5) given by $\{1, e^{i\phi}, e^{-i\phi}\}$. Then, from the general expression of the homography, it can be deduced that $\mathbf{n} = (0, 0, -1)^T$ and relative motion up to scale $(x, y, 0)^T$ analogue as the assumptions defined for the homography parametrization. In this case, the robots are in formation with all the homographies induced by pairs of robots equal to the homography computed from all the robots (5).

In the second case, the motion of the robots is not rigid, and they are not in the desired configuration. Then, the computation of the homography gives a matrix of the form

$$\mathbf{H}_{nonrigid} = \begin{bmatrix} s \cos \phi & s \sin \phi & h_{13} \\ -s \sin \phi & s \cos \phi & h_{23} \\ 0 & 0 & 1 \end{bmatrix}, \quad (6)$$

where the upper left hand 2×2 matrix is no longer orthogonal. This previous matrix corresponds to a similarity transformation, i.e. translation, rotation and isotropic scaling represented by the scalar s . Angles and ratios of lengths are invariants by this transformation. The eigenvalues of this similarity are $\{1, s e^{i\phi}, s e^{-i\phi}\}$ and encapsulate the rotation angle. Comparison with the general expression of the homography leads again to $\mathbf{n} = (0, 0, -1)^T$ but to a computed relative motion $(x, y, (s-1)d^2)^T$ up to scale, with $z \neq 0$. Therefore, the nonrigid motion of the robots induces a valid homography but not constrained to the assumed camera motion. We need to define a desired homography like $\mathbf{H}_{nonrigid}$, but being induced by a motion that keeps the camera motion constraints. This can be done normalizing (6) to make the upper left hand 2×2 matrix orthogonal and setting $h_{33} = 1$ to hold the planar motion constraint of the camera ($z = 0$). Alternatively, we can simply normalize the upper left hand 2×2 matrix and obtain the desired homography with

$$\mathbf{H}^d = \mathbf{H}_{nonrigid} \begin{bmatrix} 1/s & 0 & 0 \\ 0 & 1/s & 0 \\ 0 & 0 & 1 \end{bmatrix}, \quad (7)$$

where s is computed as the norm of the upper left hand 2×2 matrix of $\mathbf{H}_{nonrigid}$. Then, the goal is to control the robots in such a way that all the homographies are led to \mathbf{H}^d to reach the desired configuration.

The $\mathbf{H}_{nonrigid}$ relates each point \mathbf{p} of the current image with the corresponding point \mathbf{p}' in the desired formation image with $\mathbf{p}' = \mathbf{H}_{nonrigid} \mathbf{p}$. The desired homography \mathbf{H}^d is used now to define the goal location of the points in the image as $\mathbf{p}^d = (\mathbf{H}^d)^{-1} \mathbf{p}'$. Notice that the desired location of the robots in the image computed from the desired homography is not constant and varies along the time depending on the motion of the camera and the robots.

III. VISUAL CONTROL LAW

From the desired homography computed as explained in the previous section, we propose a control scheme to drive the robots to the desired configuration defined by an image

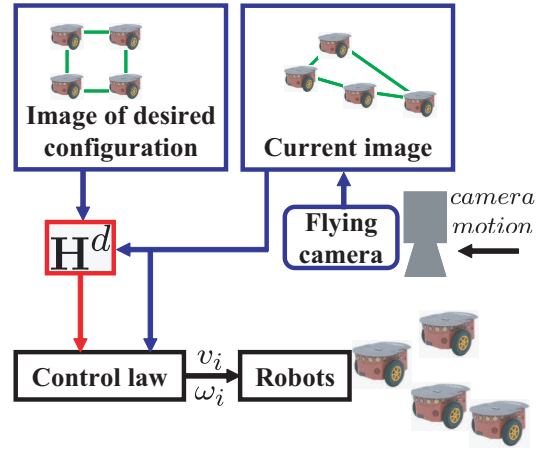


Fig. 2. Overview of the control loop. In each iteration of the control, the flying camera takes a current image of the robots, the desired homography \mathbf{H}^d is obtained and used in the control law to compute the robot velocities necessary to reach the desired configuration of the multi-robot system.

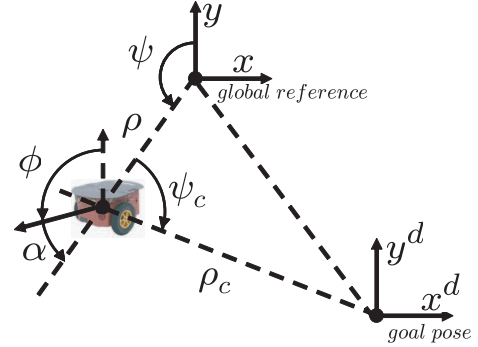


Fig. 3. Coordinate systems from a top view of the 3D scene. The robot position is given by $(x, y, \phi)^T$ or $(\rho, \alpha, \phi)^T$ in the global reference. The different parameters depicted are described along the text.

of that configuration. An overview of the control loop is depicted in Fig. 2.

A. Robot Model and Coordinate Systems

Different coordinate systems defined in the 3D space are depicted in Fig. 3. The state of each robot is given by $(x, y, \phi)^T$, where ϕ is the orientation of the robot expressed as the angle between the robot body y -axis and the world y -axis. Each robot has two velocity inputs, the linear velocity v and angular velocity ω , with v in the direction of the robot y -axis, and ω about the robot z -axis. The kinematics of each robot can be then expressed in general in polar or Cartesian coordinates in a fixed reference as

$$\begin{cases} \dot{\rho} = v \cos \alpha \\ \dot{\alpha} = \omega - \frac{v}{\rho} \sin \alpha \\ \dot{\phi} = \omega \end{cases}, \text{ and } \begin{cases} \dot{x} = -v \sin \phi \\ \dot{y} = v \cos \phi \\ \dot{\phi} = \omega \end{cases}, \quad (8)$$

respectively, being

$$x = -\rho \sin \psi \quad \text{and} \quad y = \rho \cos \psi. \quad (9)$$

The alignment error α is defined as the angle between the robot body y -axis and the distance vector ρ ,

$$\alpha = \phi - \psi. \quad (10)$$

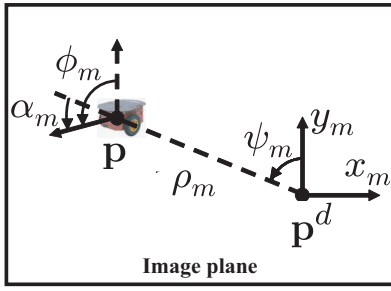


Fig. 4. Coordinate systems on the image plane for each robot. Subindex m denotes that the variable is defined on the image plane (the same variable without subindex m refers to the 3D space). Point \mathbf{p} is the image projection of a robot and \mathbf{p}^d its location to reach the desired configuration of the multi-robot system.

We now introduce several variables, depicted in Fig. 4, to define the state of each robot on the image plane with (ρ_m, ψ_m, ϕ_m) . The origin of the coordinate system for each robot \mathbf{p} on the image plane is placed in the desired location \mathbf{p}^d , i.e. the robots are in the desired configuration when all of them are in the origin of their respective references (\mathbf{p}^d).

The variable ρ_m denotes the distance of the projection of a robot in the image \mathbf{p} with respect to its desired position on the image \mathbf{p}^d , and so

$$\rho_m = \sqrt{(p_x - p_x^d)^2 + (p_y - p_y^d)^2}, \quad (11)$$

and also

$$\psi_m = \text{atan2}(- (p_x - p_x^d), (p_y - p_y^d)), \quad (12)$$

where function atan2 returns the value of the arc tangent using the sign of the arguments to determine the quadrant. ϕ_m can be computed directly from the image of the robot with computer vision techniques or estimated with $\phi_m = \text{atan2}(-\Delta p_x, \Delta p_y)$, where Δp_x and Δp_y is the incremental motion of the robot in the image plane. The alignment error on the image α_m is also defined as $\alpha_m = \phi_m - \psi_m$.

B. Control Law

The definition of the control law consists of three sequential steps with their respective controllers for each robot. The first controller is a pure rotation that turns the robots in such a way that they finally point to their desired positions. This controller is defined as

$$\text{Step 1} \begin{cases} v = 0 \\ \omega = \dot{\psi}_c - k_\omega (\alpha_m - \pi) \end{cases} \quad (13)$$

being $k_\omega > 0$ a control gain, and ψ_c is defined as the angle with vertex at the robot position and leads to the goal position and the global reference (Fig. 3). The value of the alignment error α_m is measured directly in the image plane, while $\dot{\psi}_c$ can be estimated with an observer. The goal of the second step is to reach the desired position up to orientation. This second controller is defined as

$$\text{Step 2} \begin{cases} v = \dot{\rho}_d - k_v \rho_m \\ \omega = \dot{\psi}_c - k_\omega (\alpha_m - \pi) \end{cases} \quad (14)$$

being $k_v > 0$ a control gain. The term $\dot{\rho}_d$ is related with the variation of the distance ρ_c because of the goal location displacement, and it is defined as $\dot{\rho}_d = \partial \rho_c / \partial \mathbf{x}^d$, with $\mathbf{x}^d(t) = (x^d, y^d, \phi^d)^T$. This parameter can be estimated with an observer. The image projection of the distance to the desired position ρ_m is measured directly in the image plane. The rotational velocity is defined the same as in the first controller. In general, we can assume that the motion of the mobile robots is smooth and we may consider in practice the values of $\dot{\rho}_d$ (13) and $\dot{\psi}_c$ (14) negligible, and they are not used in the computation of the control velocities in the experiments.

After the second step, the robots are in formation and only a pure rotation is needed to reach the desired configuration for the robot formation. The controller for the third step is defined as

$$\text{Step 3} \begin{cases} v = 0 \\ \omega = -k_\omega ((\phi_m - \psi_{Fm}) - (\phi_m^0 - \psi_{Fm}^0)) \end{cases} \quad (15)$$

where ψ_{Fm} is a representative angle of the robot formation and it is used to define the relative angles of the robots within the formation. The parameter ψ_{Fm} is defined for any pair of robots (i, j) with $i \neq j$ as

$$\psi_{Fm}^{ij} = \text{atan2}(-(p_x^i - p_x^j), (p_y^i - p_y^j)). \quad (16)$$

The superindex ij has been removed in (15) and hereafter for ease of the notation. The superindex 0 in ϕ_m^0 or ψ_{Fm}^0 refers to their corresponding values in the reference image.

C. Stability Analysis

In the following, the stability of the control scheme is analyzed for each step by means of the *Lyapunov's Direct Method*.

1) *Step 1*: The robots perform a pure rotation ($v = 0$), and we define the Lyapunov function and its derivative as

$$V = (\alpha - \psi_c - \pi)^2 / 2 \quad (17)$$

$$\dot{V} = (\alpha - \psi_c - \pi)(\omega - \dot{\psi}_c) \quad (18)$$

Developing this expression with the value of ω , and assuming that $\dot{\psi}_c$ is correctly estimated, we obtain

$$\dot{V} = -k_\omega (\alpha - \psi_c - \pi)(\alpha_m - \pi). \quad (19)$$

Notice that α_m is the image projection of $(\alpha - \psi_c)$ and both multiplying terms in \dot{V} has the same sign yielding $\dot{V} < 0$. Therefore, \dot{V} is negative definite and the control in the first step is asymptotically stable.

2) *Step 2*: The following candidate Lyapunov function is defined for the second step:

$$V = (\rho_c)^2 / 2 + (\alpha - \psi_c - \pi)^2 / 2. \quad (20)$$

We consider the analysis of the local stability in the second step given $\alpha_m = \pi$ (i.e. $\alpha - \psi_c = \pi$) after the first step. Therefore

$$V = (\rho_c)^2 / 2 = (x - x^d)^2 / 2 + (y - y^d)^2 / 2, \quad (21)$$

and its derivative is

$$\begin{aligned}
\dot{V} &= \rho_c \dot{\rho}_c & (22) \\
&= (x - x^d)(\dot{x} - \dot{x}^d) + (y - y^d)(\dot{y} - \dot{y}^d) \\
&= v \left(-(x - x^d) \sin \phi + (y - y^d) \cos \phi \right) \\
&\quad - (x - x^d)\dot{x}^d - (y - y^d)\dot{y}^d \\
&= v \rho_c - \dot{\rho}_d \rho_c
\end{aligned}$$

with $(\dot{\rho}_d \rho_c) = (x - x^d)\dot{x}^d + (y - y^d)\dot{y}^d$. The previous expression has been developed taking into account that $(\alpha - \psi_c = \pi)$ and then $\tan \phi = -(x - x^d)/(y - y^d)$. Assuming that $\dot{\rho}_d$ is correctly estimated, we obtain $\dot{V} = -k_v \rho_c \rho_m < 0$ and the control in the second step is locally asymptotically stable.

3) *Step 3:* The robot performs a pure rotation to get the desired relative orientation of the robots in the formation. The Lyapunov function and its derivative are defined as

$$V = (\phi - \psi_F - \phi^0 + \psi_F^0)^2 / 2 \quad (23)$$

$$\begin{aligned}
\dot{V} &= (\phi - \psi_F - \phi^0 + \psi_F^0) \omega & (24) \\
&= -k_\omega (\phi - \psi_F - \phi^0 + \psi_F^0) (\phi_m - \psi_{Fm} \\
&\quad - \phi_m^0 + \psi_{Fm}^0)
\end{aligned}$$

It can be seen that both multiplying terms of \dot{V} correspond to the rotational error with the same sign. Therefore, \dot{V} is negative definite and the control in the third step is asymptotically stable.

The motion of each robot is not independent of the rest of the team, but related through the homography by the definition of the desired configuration. Given that the desired configuration is involved in the stability analysis of each individual robot, their individual convergence implies the convergence of the global system.

IV. EXPERIMENTS

In this section, several simulations showing the performance of the control scheme are presented. The virtual environment of the experiment assumes that the projection of the robot in the images can be detected and identified in order to match each robot with its correspondence in the other images. The results of two different experiments using the three-step control scheme, (13)-(15), are shown in Fig. 5 and Fig. 6. The first one considers four robots in a square formation while the flying camera undergoes a circular motion. In the second experiment, six robots are set in a triangular configuration, while the flying camera moves with sinusoidal velocities. In both cases, the motion of the camera and the robots, as well of the evolution of different variables are depicted. The figures of the top view show the robots in the desired configuration as well as the initial position of the robots and their evolution under the control law for reaching the desired configuration. It can be seen that the desired configuration (i.e. the relative positions between the robots in the formation) is reached correctly, independently of camera motion or the absolute position of the robot team. In the last part of the simulations, the angular velocities show a peak due to the execution of the last step

of the control scheme (15). This step ensures that the final orientation of the robots agrees with the desired multi-robot configuration. Depending on the application, if the goal is to reach the desired formation independently of the robot's orientation, this last step is optional. For example, the case of considering a secondary task performed by robots having omnidirectional capabilities. The evolution of the homography entries is also depicted in Fig. 5 and Fig. 6. It can be seen that all the individual homographies computed between each pair of robots converge to the desired homography. Notice that the desired homography is not constant, as it evolves depending on the motion of the camera. The results show good performance of the homography-based control scheme. More examples are given in the **video** attachment.

V. CONCLUSION

A new control scheme has been proposed to lead a group of robots to a desired configuration. The control law is based on a particular homography parametrization that allows to define the desired location of the robots in the image plane. The advantages of this approach are the simplicity of the definition of any arbitrary desired configuration for the set of robots avoiding the need of metric information on the 3D space as well as the control law does not need to know the motion of the flying camera. In fact, the control performance is independent of the camera motion and the camera is able to perform additional tasks simultaneously. The validity of the approach is supported by the stability analysis and simulations, which show the effectiveness of the approach.

REFERENCES

- [1] A. K. Das, R. Fierro, V. Kumar, J. P. Ostrowski, J. Spletzer, and C. J. Taylor, "A vision-based formation control framework," *IEEE Transactions on Robotics and Automation*, vol. 18, pp. 813–825, 2002.
- [2] R. Vidal, O. Shakernia, and S. Sastry, "Following the flock: Distributed formation control with omnidirectional vision-based motion segmentation and visual servoing," *Robotics and Autonomous Magazine*, vol. 11, no. 4, pp. 14–20, 2004.
- [3] J. Chen, D. Sun, J. Yang, and H. Chen, "Leader-Follower Formation Control of Multiple Non-holonomic Mobile Robots Incorporating a Receding-horizon Scheme," *The International Journal of Robotics Research*, vol. 29, no. 6, pp. 727–747, 2010.
- [4] F. Chaumette and S. Hutchinson, "Visual servo control, part I: Basic approaches," *IEEE Robotics and Automation Magazine*, vol. 13, no. 4, pp. 82–90, Dec. 2006.
- [5] H. Chen, D. Sun, and J. Yang, "Global localization of multirobot formations using ceiling vision SLAM strategy," *Mechatronics*, vol. 19, no. 5, pp. 617 – 628, 2009.
- [6] G. López-Nicolás, J. J. Guerrero, and C. Sagüés, "Visual control of vehicles using two-view geometry," *Mechatronics*, vol. 20, no. 2, pp. 315 – 325, 2010.
- [7] G. Blanc, Y. Mezouar, and P. Martinet, "Indoor navigation of a wheeled mobile robot along visual routes," in *IEEE International Conference on Robotics and Automation*, April 2005, pp. 3365–3370.
- [8] J. Courbon, Y. Mezouar, and P. Martinet, "Indoor navigation of a non-holonomic mobile robot using a visual memory," *Autonomous Robots*, vol. 25, no. 3, pp. 253–266, 2008.
- [9] G. López-Nicolás, N. R. Gans, S. Bhattacharya, J. J. Guerrero, C. Sagüés, and S. Hutchinson, "Homography-based control scheme for mobile robots with nonholonomic and field-of-view constraints," *IEEE Transactions on Systems, Man, and Cybernetics, Part B*, vol. 40, no. 4, pp. 1115–1127, 2010.
- [10] R. I. Hartley and A. Zisserman, *Multiple View Geometry in Computer Vision*, 2nd ed. Cambridge University Press, 2004.

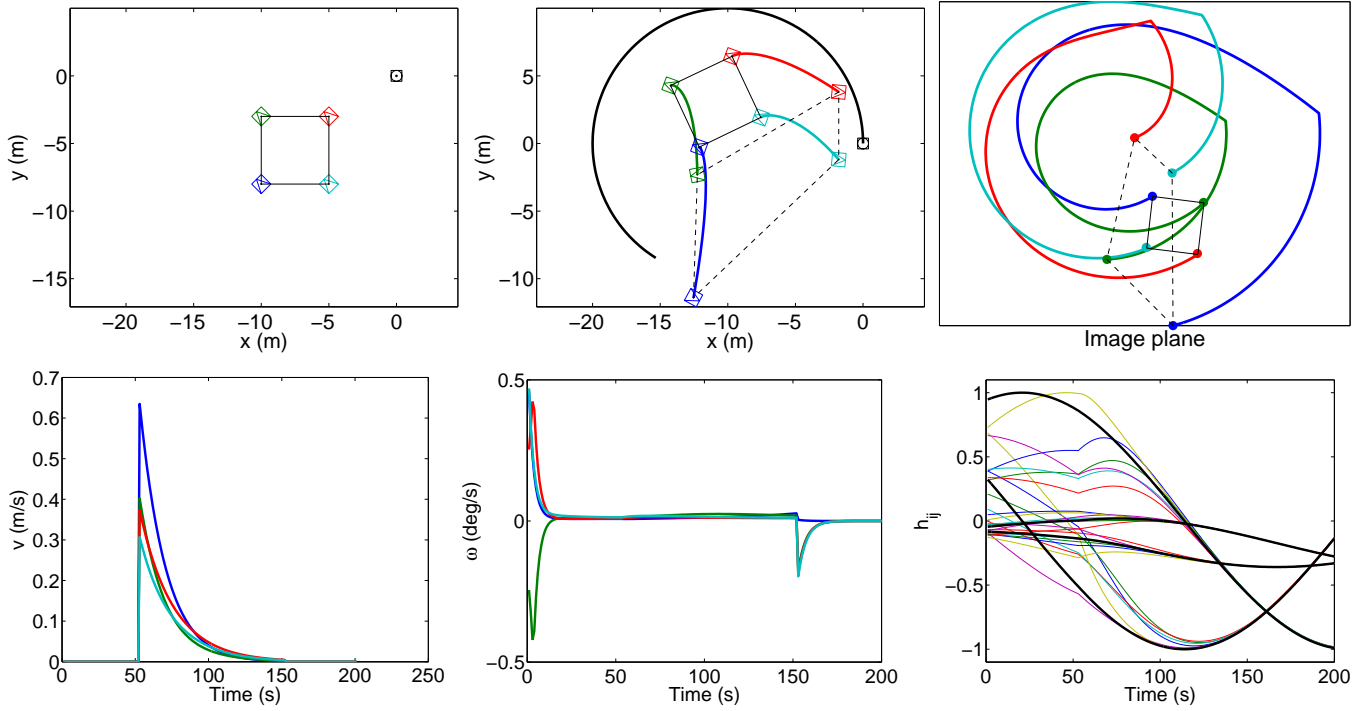


Fig. 5. Simulation with the flying camera undergoing a circular motion. The robots are initially in an arbitrary configuration and the goal is to reach the desired one. Top-left: Desired configuration for 4 robots in square formation. Top-middle: top view of the camera (the initial position is depicted with a circle inside a square) and the robots. The initial configuration is drawn with dashed line and the path followed by the robots to reach the desired configuration is shown (thick lines). Top-right: trace of the robots in the image plane. Second row: linear and angular velocities of the robots, and evolution of the homography entries (h_{11} , h_{12} , h_{13} , h_{23}) of the desired homography (thick lines) and the current homographies between the robots (thin lines).

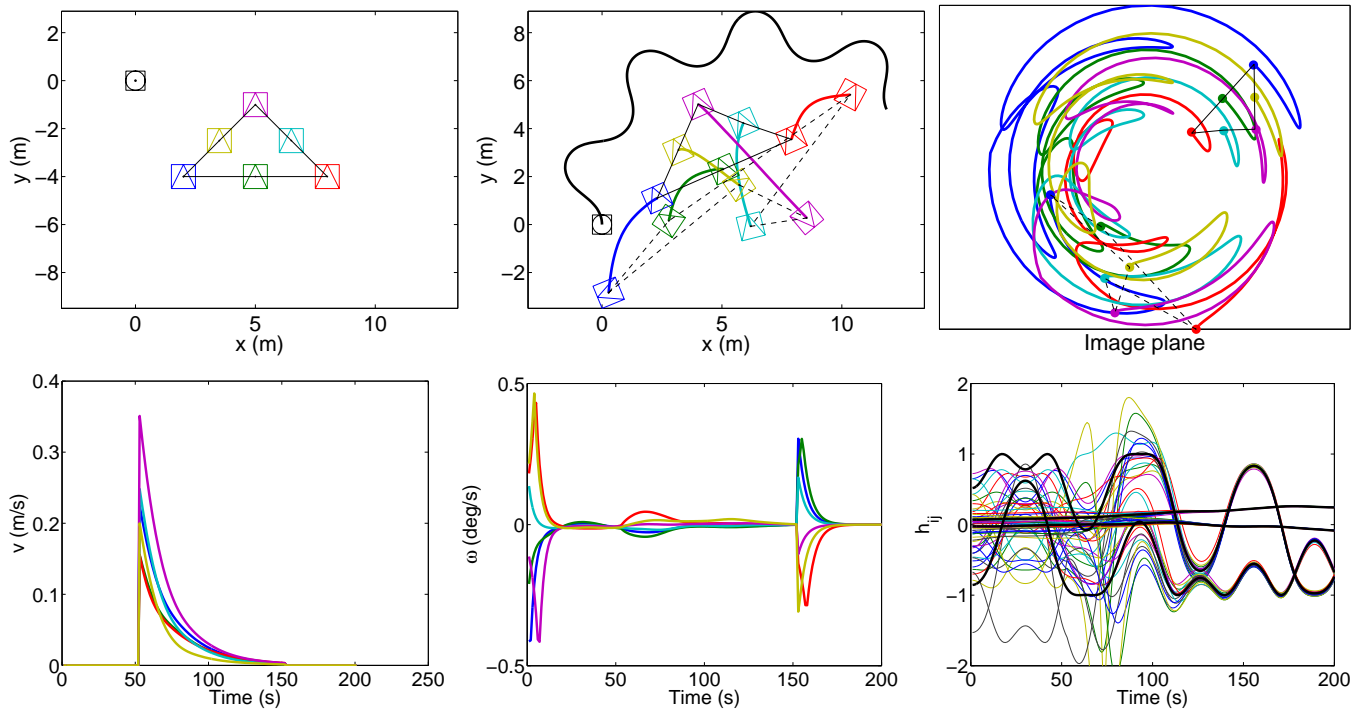


Fig. 6. Simulation with the flying camera undergoing a motion compounded of sinusoids. The robots are initially in an arbitrary configuration and the goal is to reach the desired one. Top-left: Desired configuration for 6 robots in triangular formation. Top-middle: top view of the camera (the initial position is depicted with a circle inside a square) and the robots. The initial configuration is drawn with dashed line and the path followed by the robots to reach the desired configuration is shown (thick lines). Top-right: trace of the robots in the image plane. Second row: linear and angular velocities of the robots, and evolution of the homography entries (h_{11} , h_{12} , h_{13} , h_{23}) of the desired (thick lines) and the current homographies between the robots (thin lines).